ARTICLE   **OPEN ACCESS**

SENSITIVE LOAD SENSOR BASED ON PIEZORESISTIVE PROPERTIES OF MULTI-WALLED CARBON NANOTUBE

Mohammadmehdi Choolaei[2], Milad Nazarzadeh[1], Amir Yadegari[1], Hakimeh Zali[1], Fatemeh Yazdian[3], Meisam Omidi[1*]

[1]*Medical Nano-Technology & Tissue Engineering Research Center, School of Advanced Technologies in Medicine, Shahid Beheshti University of Medical sciences, Tehran, IRAN*
[2]*Department of Tissue Engineering and Regenerative Medicine, School of Advanced Technologies in Medicine, Shahid Beheshti University of Medical sciences,Tehran, IRAN*
[2]*Research Institute of Petroleum Industry (RIPI), Azadi sport complex West Blvd., Tehran, IRAN*
[3]*Faculty of New Science and Technology, University of Tehran , Tehran, IRAN*

ABSTRACT

The fabrication of a micro-electro-mechanical systems (MEMS) piezoresistive load sensor is reported. The sensor has the shape of a cantilever beam on a paper substrate. Printable multi-walled carbon nanotube (MWCNT) ink was fabricated to be used as a sensing component, because of its excellent piezoresistive and electromechanical properties.. The results show that using MWCNT ink with proper sonication duration can result in a considerable force range and gauge factor for the fabricated sensor, which are two important designing factors. The results illustrated a linear resistance change with the applied forces. The force range, force resolution, and sensitivity were found to be 25 mN, 60 µN, and 1.6 mV mN-1, respectively. Furthermore, the effects of sonication time, number of printing, and temperature on the ink resistance are experimentally studied. Finally, in order to decrease the noise levels monolithic integration of a signal-processing circuit was used. This sensor is inexpensive, simple to fabricate, light-weighted, and disposable.

*****Corresponding author: Email:** m_omidi@sbmu.ac.ir

INTRODUCTION

Carbon nanotubes (CNTs) exhibit unique structural, electromechanical, and thermal properties as well as their nanometer scale diameter and high aspect ratio, which make them ideal sensing components in applications for load and strain sensors [1]. When CNTs are subjected to mechanical deformations, their resistance varies due to the applied changes in their band structures. This matter implies the potential use of CNTs as sensing component in piezoresistive load sensors. Both individual single-walled carbon nanotubes (SWCNTs) and multi-walled carbon nanotubes (MWCNTs) were found to show a repeatable load–unload relationship between their mechanical deformation and their electromechanical properties [2-5].

A review paper by Obitayo and Liu, has presented some important features of CNTs for strain sensing [6]. Dharap et al. have used pure SWCNT films (bulky paper) as sensing component in strain sensors [7]. In addition, CNT composite films can also be used for strain sensing. For example, Pham et al. have fabricated a poly (methyl methacrylate)/MWCNT composite film based sensor [8]. Also, a new type of polyisoprene/MWCNT composite strain sensor was reported by Knite et al., Kang et al., and Loh et al., which have cited the use of CNT/polymer composites as strain sensors for structural health monitoring [9-11]. Moreover, Li et al. have proposed a freestanding MWCNT film (bulky paper) as a strain sensor [12]. In 2011, two outstanding studies on stretchable carbon nanotube strain sensors were conducted by Yamada et al. and Lipomi et al., which claimed to facilitate the detection of human interaction, human-motion, and biofeedback [13,14].

In the commercial micro-electro-mechanical systems (MEMS) products, silicon materials are used as conventional substrates and microfabrication processes are used as manufacturing approaches, which all require access to cleanroom equipment [15]. Although silicon based MEMS products show excellent performance, both materials and fabrication processes are expensive. Another alternative for sensor substrate is polymer composites. In Spite of recent attempts to use polymer materials (e.g. polydimethylsiloxane, polyethersulfone) as flexible substrates [16-20], the costs of these materials and complex fabrication process have restricted their applications. Recently, paper has drawn much interest as a new alternative technology for fabricating simple, low-cost, portable, and disposable analytical devices for many applications [21-25]. In 2011, Liu et al. reported the fabrication of a paper-based piezoresistive force sensor [26]. In order to measure force, they took advantage of the piezoresistive effect generated by graphite ink as a conductive material that was patterned on a paper substrate. After that, Ren et al. suggested a paper-based Piezoresistive sensor based on Liu et al. work [27]. In this work, graphite was used as sensing component, and they tried to develop a less expensive fabrication process than the previous work; for example, they substituted silver ink for contact pads to copper foil.

Here in this paper, we have developed a new high-performance paper-based load sensor by using MWCNT ink as a sensing component, which is an excellent piezoresistive material. Printable MWCNT and silver inks were fabricated, and the electrical properties of MWCNT ink were studied. In order to reduce time, cost, and waste during fabrication, also increasing reliability, repeatability, and sensitivity of the sensor, inkjet printing process was used to create electrical circuits onto the paper. Basic parameters of MWCNT/paper load sensor, e.g. rang of linearity, sensitivity, and force resolution were measured. The effects of sonication time, number of printing, and temperature on the ink resistance were investigated. This load sensor is inexpensive, simple to fabricate, light-weighted, and disposable. Due to these characteristics, this sensor can be recognized as an appropriate single-use device in analytical applications such as medical diagnostics.

MATERIALS AND METHODS

Principle of Paper-based Load Sensor

Piezoresistivity is a common sensing principle for many micromachined sensors. The main principle of sensors like this is using the piezoresistive effect of the sensing components. In this study, MWCNT was used as sensing component, and the paper-based sensors were formed in the shape of cantilever beams, using a laser cut. In addition, the conductive components were printed using a HP Deskjet 1600CN printer. By applying a concentrated force at the free end of the cantilever beam and measuring the change in the resistance of the sensing component, as a result of deflection, it was possible to calculate the quantity of the applied load (see Supplementary Information for details regarding the designed setup for measurement).

Inkjet Printing Process

For obtaining printable inks from different particles, e.g. CNTs and silver powder, the listed factors should be considered. (1) The diameter of the particles should be less than 1/100 the size of the nozzle diameter, if not nozzle clogging would normally happen [28]. (2) Ink viscosity, affecting the formation of drops, should be in the range of 2-30 mPa s [29]. (3) Ink surface tension, dictating the spherical shape of the liquid drops coming from the nozzle, should be up to 60 mN m−1 for reaching an acceptable printing process [29]. Inks with high surface tension may not wet or travel through the cartridge assembly, which results in a clogging or irregular printing. On the other hand, low surface tension can lead to an ink leakage from the cartridge and may make the print head to flood during the printing process. (4) Stability is an essential factor to achieve a suitable ink. Different methods are used for obtaining inks with high stability such as: (i) placing functional groups like carboxyl ($(CO_2H)n$) on the surface of the particles, (ii) using different dispersion methods (e.g. ultrasounds or flow impingement) [29], (iii) using different surfactants like pluronic F127 (triblock co-polymer) [28], methanesulfonic acid [30], dioctyl sodium sulfosuccinate [30], poly(N-vinyl-2-pyrrolidone) [30], and polyelectrolytes [31]. The appropriate stability time for an ink is about one week at room temperature, which in this period the particles should not settle or agglomerate [29].

MWCNT Ink Preparation

For obtaining an efficient dispersion of CNTs in the solvent, the hydrophobic surface of the nanotubes needs to be changed to a hydrophilic surface by attaching polar groups such as carboxyl,interacting with solvent molecules and forming hydrogen bonds. It is important to know that CNT ink is not a true solution; therefore, CNT ink can be described as a colloidal suspension, which is either stable (colloid) or sediments with time (suspension) depending on the CNTs concentration. In order to prepare CNT ink, a suspension including the following material should be prepared: functionalized MWCNTs ($MWCNT-(CO_2H)n$) , distilled water as solvent, IPA and DEG as co-solvents, and CTAB as surfactant. MWCNTs used in this study were produced by Research Institute of Petroleum Industry (RIPI) through the chemical vapor deposition (CVD) method. They were characterized by an average diameter of

10-50 nm, length of 1-3 μm, and carbon purity of 96%. IPA, DEG, and CTAB were purchased from Merk. Details regarding the process of fabricating a printable MWCNT ink are mentioned in the Supplementary Information.

Silver Ink Preparation

In order to prepare the silver ink, Ag powder was purchased from American Elements with the characteristics of powder particle sizes average in the range of 10-50 microns and electrical resistivity of 1.586 μΩ cm. Because Ag powder was not functionalized, it was crucial to use an appropriate surfactant in order to have a stable ink. Same as the work done by Kosmala et. al. [28], pluronic F127 was used as surfactant in the silver ink. F127 is a triblock co-polymer, which comprises poly ethylene oxide (PEO) and poly propylene oxide (PPO) sections organized in a PEO–PPO–PEO arrangement. One of these sections is hydrophilic (PEO) and the other is hydrophobic (PPO). The hydrophobic Ag particles are encapsulated by the PPO section. These encapsulated particles are covered by a layer of free PEO, which helps the Ag particles to remain stable [32]. Same as CNT ink, distilled water was used as solvent and both IPA and DEG as co-solvents (see Supplementary Information for the process of silver ink preparation).

Sensor Fabrication Process

In order to prepare the cantilever beam, an A4 paper with a thickness of 340 μm was chosen as the substrate and it was patterned to the required dimensions (44.5 mm × 7.7 mm) using a laser cut with a precision of 0.12 mm. In the next step, MWCNT ink was printed at the initial section of the cantilever beam using a HP Deskjet 1600CN printer. The electrical contact pads were printed using the fabricated silver ink. In order to certify the connections between the printed contact pads and sensing component (MWCNT ink) a small drop of silver ink was placed on the connections using a painting brush. At the end, by connecting the contact pads to the multimeter (Keithley 2400 source meter), it was possible to read the resistance change of the system. A simple illustration of the final cantilever beam sensor can be observed in Figure 1.
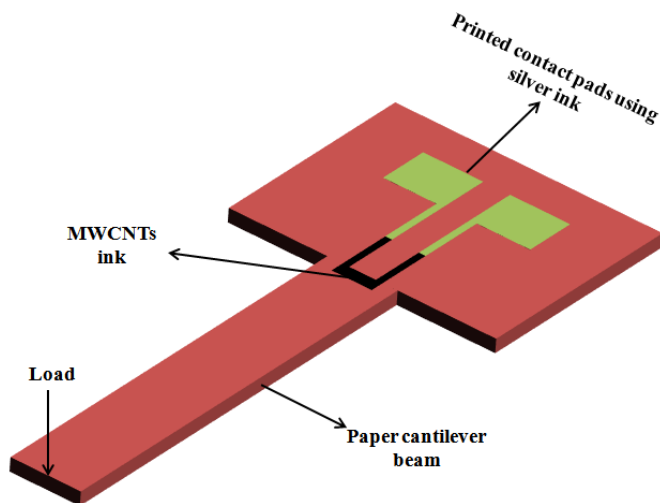

Fig. 1: Schematic view of a paper-based cantilever beam load sensor using a MWCNT resistor as the sensing component cantilever beam

....

RESULTS

Sensor Mechanical Analyses

At first, we determined the stiffness of the paper beam by applying forces as a function of deflection to the free end of the beam (Figure 2a). As the results demonstrated, the stiffness of the paper beam was about 2 GPa. Then the Young's modulus of the beam was calculated by Equation 1:

$$E = 4FL^3 / \delta WH^3 \tag{1}$$

Here the young's modulus is shown by E, the applied force to the end of the beam is presented by F, the deflection by δ, and the length, width, and thickness of the paper beam are shown by L, W, and H, respectively. By applying Equation 1, the young's modulus calculated for the paper beam was about 2 GPa, which is much lower than that of silicon (130-170 GPa) [26].

Moreover, COMSOL Multiphysics 4.2 finite element software was used for extracting the stress distribution, in order to determine the location of the connections on the sensor. The number of elements for modeling the sensor was about 1200, which gave sufficient resolution for the present simulation. Figure 2b shows the Von-Mises stress contour for the designed sensor, when a point force is applied at the free end. The induced stress on the surface is uniaxial and increases from zero at the free end to maximum at the clamped end. The stress at the clamped end is readily amplified by a constriction. Owing to the fact that we have the highest concentration of strain in the bending point (Figure 2b), unlike other works that have located the connection points on this area [26,27], we have shifted the connection between the contact pad and the sensing component to a lower point. In this way, we have decreased the effect of resistance change of silver ink, as the contact resistance, on the total resistance change of the system. The effect of silver ink on the measured resistance is explained as follows [12]:

$$R_{measured} = R_{contact} + R_{MWCNT} \tag{2}$$

The measured resistance ($R_{measured}$) includes the contact resistance ($R_{contact}$) and the resistance of MWCNT (R_{MWCNT}). As it can be seen in Equation 2, by changing the location of the connections we have eliminated the irreversible and non linier contact resistance ($R_{contact}$) in order to minimize the noise in the system.
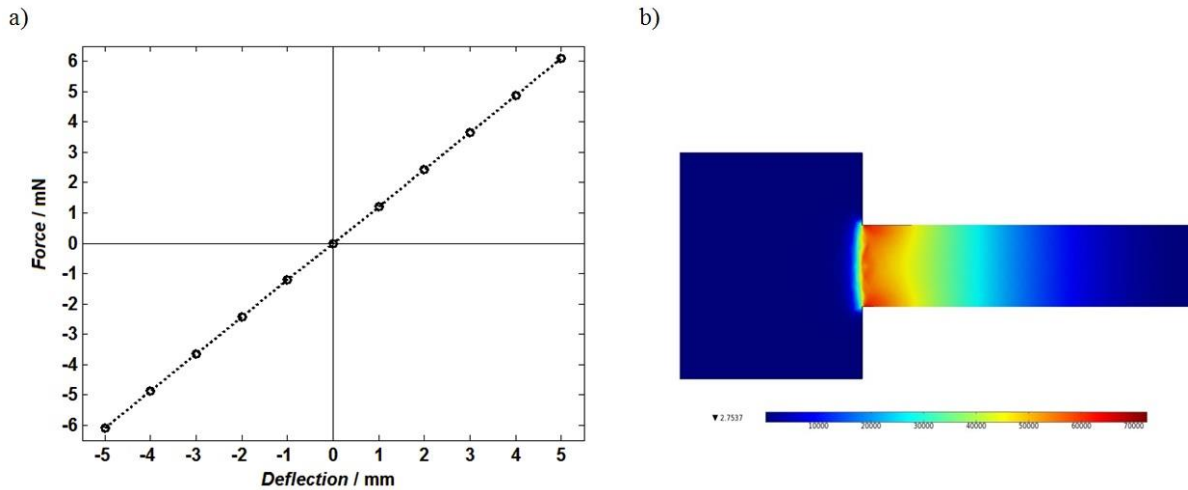
a)

b)

Fig.2: a) Calibration plot of force–deflection. b) Von-Mises stress contour calculated by finite element analyses (FEA) using COMSOL Multiphysics 4.2.

Ink Electrical Properties
The effect of sonication time, as a processing parameter, has been investigated in this work (Figure 3a). It has been observed that the resistance of the MWCNT ink significantly decreases by increasing the sonication time, as shown in Figure 3.
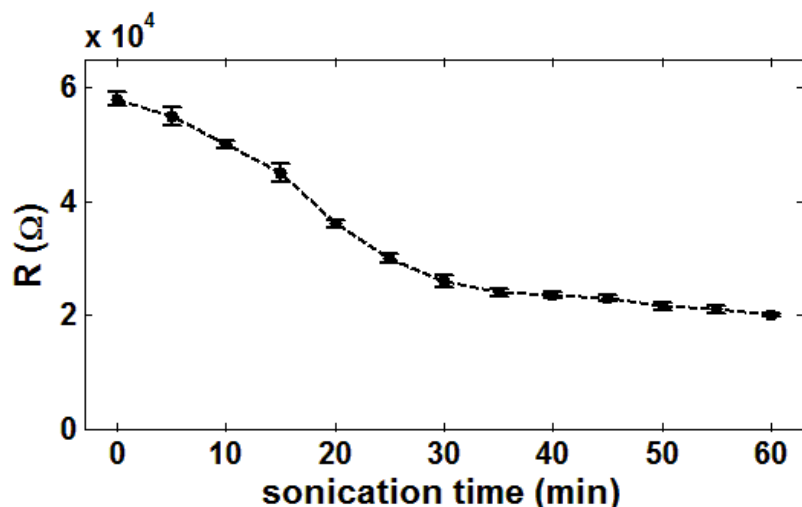
Fig. 3: The resistance values of the multi-walled carbon nanotubes ink versus sonication time.

Generally, due to the strong van der Waals interactions among individual CNTs, they are mostly observed as a group of individual tubes forming thicker ropes with longer lengths (Figure 4a). These rope structures are commonly referred to as CNT ropes, which are the usual form of the synthesized CNTs with the current synthesis processes (rather than individual tubes). It has been shown that by increasing the time and power or the sonication process, these CNT ropes can be separated to individual tubes or smaller sized ropes [33,34] (Figure 4)

By conducting the centrifugal process along with the sonication, we are actually eliminating the large ropes remaining after sonication. Hence, by continuing this process, or better to say increasing the sonication and centrifugation time, a gradual reduction in the CNT rope size (decrease in the diameter and length) can be observed (Figure 4). As will be explained later, this fall in the size of CNT ropes (shorter and thinner ropes) increases the piezoresistive sensitivity of the fabricated sensor by raising the number of inter-tube contacts, increasing the ratio of tunneling resistance to the overall resistance of the thin film [35-37].
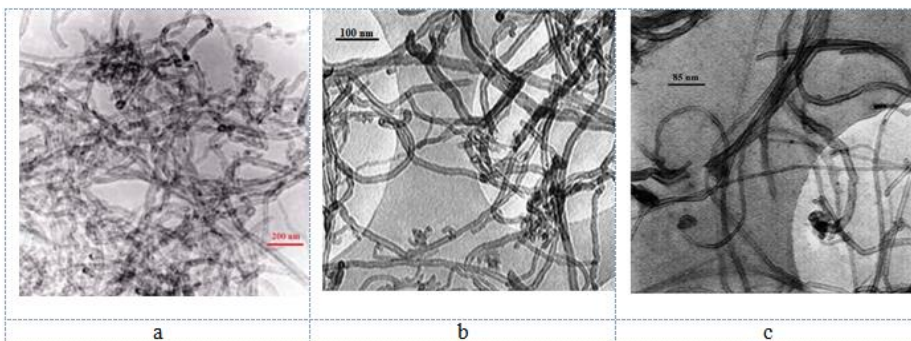

Fig. 4: TEM images of MWCNTs after a) 30 min, b) 4hr, and c)7hr sonication.

Also, the surface resistance of the MWCNT and silver deposit printed on the paper sensor are plotted versus the number of printing in Figures 5a and 5b, respectively. Based on the ASTM D-254 standard, sheet resistances were performed at room temperature. It was found that the electrical resistance drops with increasing the number of prints, as the layer of nanotubes increases in thickness and achieves the percolation threshold (after printing 12 times).
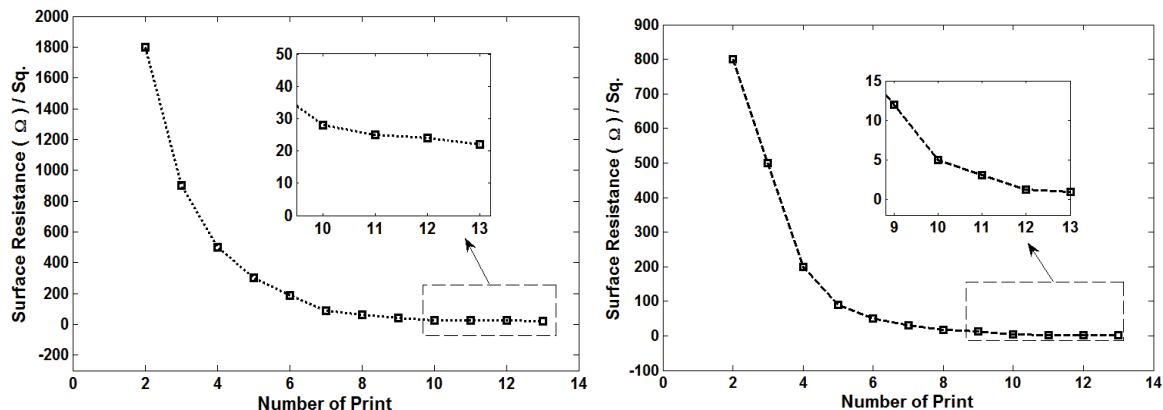
Fig. 5: a) The surface resistance versus the number of printing for MWCNT. b) The surface resistance versus the number of printing for silver.

However, gauge factor of the fabricated sensors presented different behaviors, regarding the number of printing (film thickness). Our work indicated the fact that sonication time can play a decisive role in determining the importance of this factor on the sensor's performance. As Figure 6 shows, the gauge factor of sensors fabricated using inks with low sonication time illustrated none or small dependence on the number of printing. On the other hand, by increasing the sonication duration up to about 7 hrs, reaching CNTs with shorter lengths and smaller diameters, an intense positive relation was observed between the number of printing and the sensors gauge factor. A clear understanding has not yet been reached on the mechanisms involved in the thickness-dependent piezoresistive response of the fabricated sensors; however studying Figure 6a clearly shows the compound influence of the detailed packing structure of MWCNTs. Up to now, several works have focused on studying the geometric packing of thin-rods or fibers [38-40], which in most of them rod excluded volume is considered as an important physical factor in dictating rods structure. This volume is referred to the area around a rod which is not accessible for the center of another rod. This volume is usually estimated by $dL2$, where d and L are respectively the diameter and length of the rods. According to the mentioned parameter, the number of randomly packed rods in a unit volume, rod packing density, can be approximated by $1/dL2$ [41]. Luo et al. [41] have proven the direct relation between gauge factor and packing density for large deformations. Hence, by increasing the sonication time and number of printing, we are actually increasing the packing density via decreasing the diameter and length of the CNT ropes. Figure 6b illustrates the SEM image of the packing structure of MWCNT thin fills.
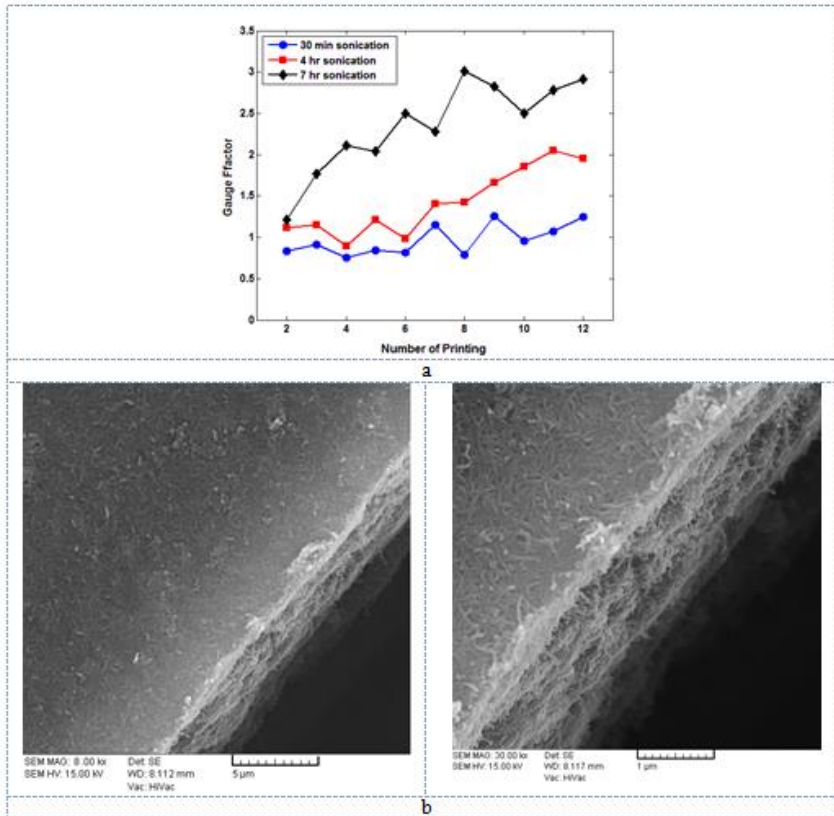
Fig. 6: a) The effect of number of printing (film thickness) and sonication duration on the gauge factor of MWCNT thin film piezoresistive sensors b) SEM image of the packing structure of MWCNT thin fills.

Figure 7a illustrates the measured voltage-current (V-I) characteristics of the MWCNTs film. The linear ohmic V-I behavior indicates the correlation between the piezoresistivity of MWCNTs and the deflection caused by the loaded force. The results determined a resistance of 20.54 kΩ for the resistors. Moreover, other factors have proved to have significant effects on the electrical resistivity of MWCNTs which we have investigated below.
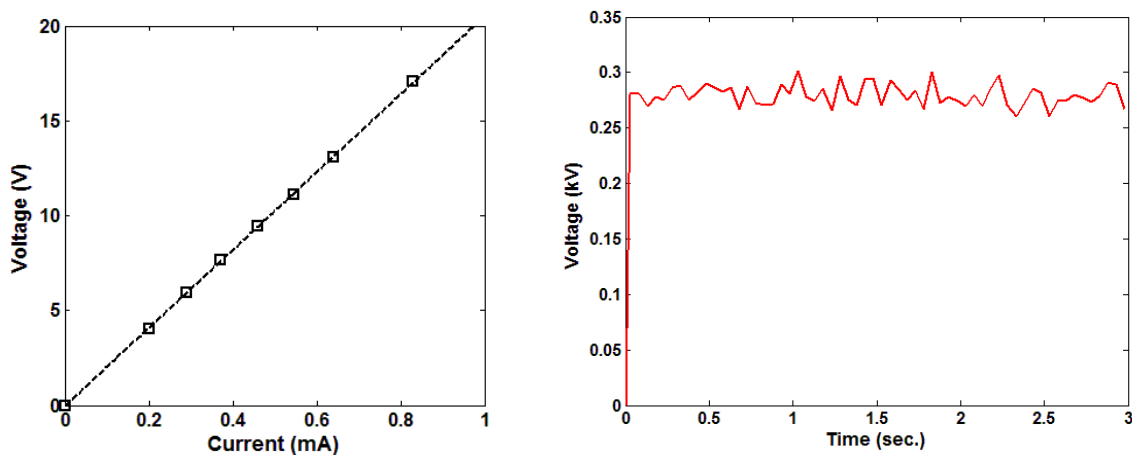

Fig. 7: a) Linear current–voltage curves for MWCNT ink resistors, showing the ohmic I–V characteristics of a good conductor. The line represents a linear fit to the experimental data with a regression equation: y = 20.54x (R² = 0.999), b) Voltage stability of the MWCNT ink under free conditions (zero load)

The output voltage of printed MWCNT ink under free load condition (zero load) is shown in Figure 7b. The input current applied to the samples under free load condition was 150 mA and as the graph shows, the output voltage of MWCNT ink took a very short time to stabilize.

Calibration

In order to perform the relation between the applied compressive strain to the free end of the paper beam (input) and the resistance change (output) of MWCNT film, we have calibrated the paper-based sensor by using a multimeter. Figure 8 presents the calculated correlation between the experimental outputs as a function of inputs for printed MWCNT ink fabricated with different sonication times. The results have illustrated a linear resistance change with the applied force/strain. By studying the calibrated results (Figure 8), the average sensitivities (kslope) of paper-based sensor with 30 min, 4h, and 7h were calculated to be 0.00017, 0.0002 and 0.0004 (mN-1), respectively. As expected, increasing the sonication time enhances the resistance change for a certain applied force/strain. Again, this matter could be explained by the positive effect of sonication time in decreasing the length and diameter of MWCNTs, leading to a raise in the packing density of the MWCNT thin film.
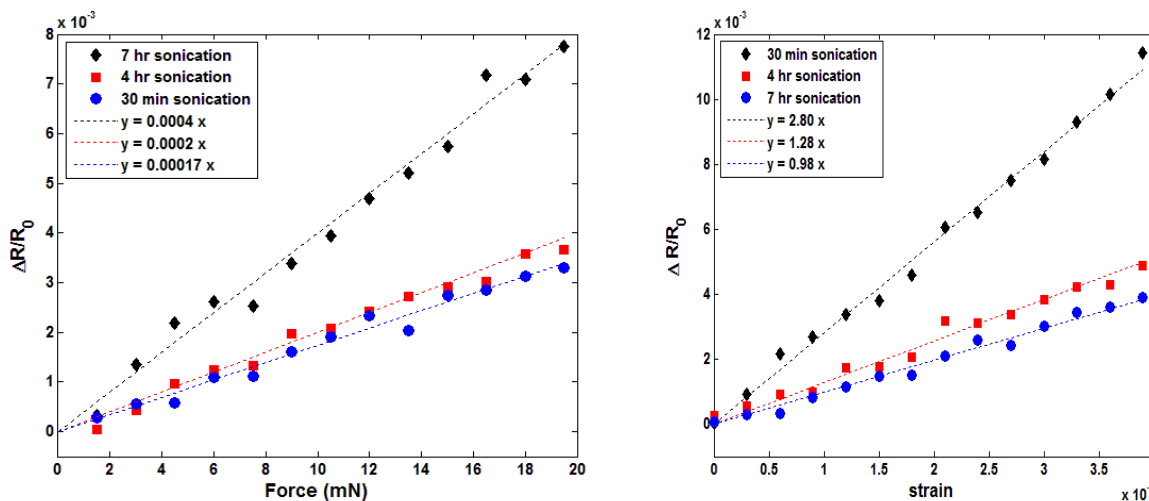

Fig. 8: Calibration plot of the output of the sensor (resistance change) as a function of applied a) force and b) strain for printed MWCNT.

Table 1 compares the measured gauge factors obtained from the fabricated sensor in this work with similar works in the field. By bearing in mind the simple fabrication process and the low price of the paper-based sensor, the presented results in Table 1 indicate an acceptable performance for the fabricated sensors using MWCNT inks with higher sonication times.

Table 1. Comparison between measured gauge factor values of CNTs sensors in different researches.

Work	gauge factor
This work (MWCNTs)	0.98 (30 min. sonication)
	1.28 (4 hr. sonication)
	2.8 (7 hr. sonication)
X Li et al. [12] (MWCNTs film)	2–3.76
Song et al. [42] (MWCNTs film)	0.01–1.25
Sickert et al. [43] (SWCNTs bundle)	2
Luo et al. [41] (SWCNTs film)	1-5

The observed piezoresistive behavior of CNTs in this study can be considered as the result of two parallel processes. First, losing the conductive channels by breaking down the existing conductive network, due to the applied strain, then forming new conductive networks due to the rearrangement in the conductive particles.

In order to analyze the behavior of CNTs under strain we first have to point out the network structure of carbon nanotubes as the main cause of the piezoresistive phenomena in this study. Carbon nanotube network consists of two

main resistances named the intrinsic, RCNT, and inter-tube. Moreover, the inter-tube resistance itself is divided into two types: the resistance caused by the tubes that are physically in contact, called the contact resistance, RC, and the resistance caused between the CNTs that are separated by a small gap which is called tunneling resistance, RT, (Figure 9) [6]. Changes in RCNTs, RTs, and RCs are closely related to the CNT network attributes, CNTs stress, positional and angular displacements of tubes, CNT volume fraction, etc. [44]. Therefore, the effect of deflection in CNTs resistance change in this study could primarily be explained by the modification in intrinsic resistance and inter-tube resistance.

Intrinsic Resistance of Carbon Nanotubes (RCNT)

Due to the one-dimensional structure of CNTs, which facilitates the electronic transport in the CNT network, they are known as materials with favorable electrical properties. It has been observed that intrinsic resistances have low values. As an example, this amount is as low as $0.2–0.4$ kΩ s µm-1 for MWCNTs [45,46]; however, they are highly sensitive to mechanical loading. As presented in different works [1,47-49], the high sensitivity of CNT can be explained by the fact that energy band gaps, which have a significant effect on CNT conductivity, are highly sensitive to the applied strain. To be more specific, the resistance of a conductive tube could be quantitatively explained by the following equations [3]:

$$RCNT\ (\varepsilon) = R0(1 + e\beta\varepsilon) \tag{3}$$
Where:
$$\beta = (1/KT)(dEgap/d\varepsilon) \tag{4}$$
$$dEgap/d\varepsilon = 3t0(1 + \upsilon)\cos(3\varphi) \tag{5}$$

R0 (kΩ) is a constant, Egap is the band gap energy, t0 is normally equal to ∼ 2.7 eV and is the tight-binding overlap integral of carbon bond C-C, φ is the chiral angle ($0<\varphi<30$), ε is the applied strain, and υ is volume concentration of CNT.

Inter-tube CNT Resistance (RC and RT)

Due to the fact that inter-tube resistance is much larger than intrinsic resistance, the conduction of CNT network cannot be only explained by studying intrinsic resistance. Inter–tube resistance is divided into two groups, the contact and tunneling resistances.

Contact resistance, RC, is defined as the resistance between the physically connected tubes. In this case, the conductions between tubes take place through electron diffusion from the connected points. Studies illustrate that contact region acts as a deciding factor in the quantitative amounts of contact resistance [50,51].

There are different factors such as extent of interfacial surface and the alignment of molecules across the interface affecting the amount of RC in a CNT network, which any modification in these parameters can change RC from a few hundred to a few thousand kΩ s [44].

On the other hand, sometimes there are no exact connections between the tubes, where conduction takes place through the small gap between the tubes using a mechanism called tunneling (Figure 9). In this case, the inter-tube resistance is called tunneling resistance, RT [52], and it can be quantitatively explained using the following equations:

$$RT = R0\ (\ e\lambda s\ ) \tag{6}$$
For small bias voltage and rectangular barrier:
$$R0\ = (1/C1)(S/k1/2) \tag{7}$$
$$\lambda = C2\ k1/2 \tag{8}$$

Constants C1 and C2 are respectively equal to C1 = 3.16 ×1010 and C2 = 1.0125, k presents the average height of the potential barrier (eV), and S equals the gap width (Å).

As it can be observed from Equations 6-8, the applied strain can modify the inter-tube resistances by widening the gaps between CNT tubes, which this matter increases the resistance in the CNT network (Figure 9).

Although both intrinsic and inter-tube resistance increase by applying a mechanical load, their extent of contributions are found to be different. In this regard, since paper (as a load transfer medium) lakes the ability to efficiently transfer the externally applied mechanical load to each individual CNT tube, the effect of RCNT on the overall piezoresistive response of CNT thin film can be neglected. On the other hand, the applied load mostly varies the gap and conductive paths between the unconnected and connected tubes, respectively. This matter leaves RC and RT mainly responsible for the piezoresistive response of the fabricated sensor. Considering the numerical and experimental studies conducted by Theodosiou et al. [53] and Luo et al. [41,54], it can be concluded that RT is the

most important factor responsible for the piezoresistivity of CNT thin film. The direct relation between the amount of packing density ($1/dL2$) and the number of conductive paths can support this idea. A decrease in the size of the CNT bundles (smaller length and diameter, higher sonication time) increases the packing density, resulting in an increase in the number of inter-tube contacts. This matter increases the effect of tunneling resistance on the overall resistance of the thin film [55,36].
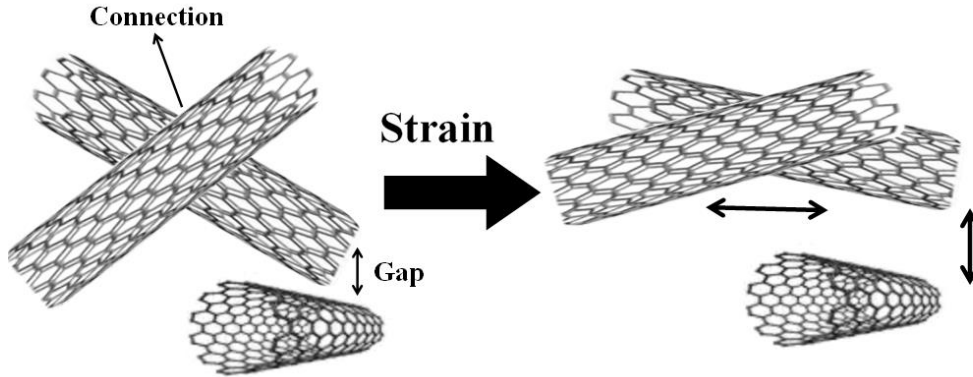

Fig. 9: Schematic of CNTs network after applying strain.

The stability of the fabricated sensor was examined through 1200 times repeated bending, Figure 10. The plotted data after each 200 cycle are the average of 5 times testing. Figure 10 depicts the change in the gauge factor of the synthesized sensor during 1200 cycles. The results illustrate a 7% increase in the gauge factor after the 1200 cyclic loading, indicating a considerable stability for the fabricated paper based sensor. This matter can be explained by the good network structures formed by the entanglement of CNT bundles/ropes and their good bonding with the paper substrate.
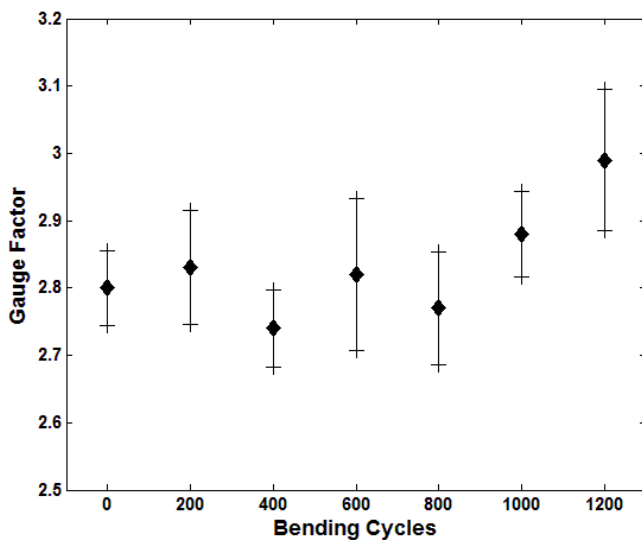

Fig. 10: Stability evaluation results for the selected MWCNT thin film sensors under 1200 cyclic tensile mechanical testing.

Moreover, the experiments revealed that there is a linear relationship between temperature and change in resistance. A raise in temperature resulted in an increase in the conductivity of the nanotube thin film as demonstrated in Figure 11. In this case, the resistance changed by 0.8 Ω for a temperature difference of 35 ˚C. According to the tunneling mechanism, electrons tend to jump from nanotube to nanotube across the gaps. With increasing the temperature these gaps expand, which makes it difficult for the electrons to jump between them. The rise in the gap lengths depends on the stiffness of the substrate. Increasing the temperature tends to reduce the stiffness of the paper, and correspondingly enlarges the tunneling gap. This enlargement of the gaps reduces the effect of the increase in electronic activities, due to the temperature rise.
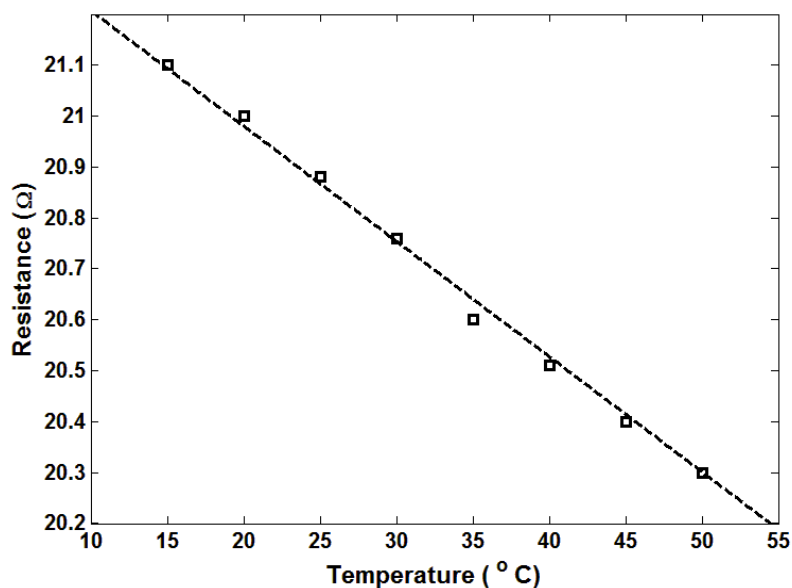
Fig. 11: Resistance as a function of temperature (from 15 ◦C to 50 ◦C).

However, the fabricated sensors have high amounts of CNTs, which elevate the number of contacts between the tubes, and decline the gap lengths. When the numbers of electrical contacts are sufficiently large, the conduction by electronic movement is dominant. Therefore, higher temperature tends to increase the electronic movement, resulting in higher electrical conductivity. This matter could also be explained by the semicunductive charge transport behavior of CNTs. The charge transport in CNT thin films is dictated by a variable-range hopping mechanism [56,57], which facilitates the charge carrier mobility and reduces the resistance at high temperature.

Monolithic Integration of a Signal-processing Circuit onto the Paper Device

Converting the change in the resistance to a more reliable signal (voltage) was done using a Wheatstone bridge circuit. However, in this study instead of using a printed circuit board (PCB) and wire-bonding for electrical connections; we have printed the conventional signal processing circuit on the paper. The structure and properties of the applied Wheatstone bridge circuit has been mentioned in the Supplementary Information. After integrating a Wheatstone bridge circuit, the sensitivity was measured to be 1.6 mV mN-1.

DISCUSSION

Research activity in the areas related to carbon nanotubes has seen phenomenal growth in the last one and half decade. In this paper, an attempt has been made to use piezoresistive property of MWCNT ink in the sensing application. We have developed a paper-based sensor on the basis of piezoresistive property of MWCNT ink for measuring the magnitude of applied loads. We have prepared MWCNT ink with these constituents: functionalized MWCNTs (MWCNT-(CO2H)n), distilled water, isopropyl alcohol (IPA), diethylene glycol (DEG), and cetyltrimethylammonium bromide (CTAB). The sensor was in the shape of a cantilever beam, which was patterned on a paper substrate (340 μm thick) using a laser cut. Our sensor has exhibited these characteristics: natural frequency of 25 Hz, force range of 0-25 mN, force resolution of 60 μN, and sensitivity of 1.6 mV mN-1. It was also found that an increase in sonication time, temperature, and number of printing resulted in a decrease in resistance. Finally, a monolithic integration of a signal-processing circuit was developed in order to decrease the footprints and noise effects.

REFERENCES

[1] Arasteh R, Omidi M, Rousta AH, Kazerooni H. p. [2011]. A study on effect of waviness on mechanical properties of multi-walled carbon nanotube/epoxy composites using modified Halpin–Tsai theory. Journal of Macromolecular Science, Part B. 50(12):2464-80.

[2] Omidi M, Alaie S, Rousta A. [2012]. Analysis of the vibrational behavior of the composite cylinders reinforced with non-uniform distributed carbon nanotubes using micro-mechanical approach. Meccanica, 47(4):817-33.

[3] Omidi M, Malakoutian MA, Choolaei M, Oroojalian F, Haghiralsadat F, Yazdian F. [2013]. A Label-Free Detection of Biomolecules Using Micromechanical Biosensors. Chinese Physics Letters. 30(6):068701.

[4] Ardjmand M, Omidi M, Choolaei M. [2015]. The effects of functionalized multi-walled carbon nanotube on mechanical properties of multi-walled carbon nanotube/epoxy composites. Oriental Journal of Chemistry. 31(4):2291-301.

[5] Zali H, Yazdian F, Omidi M. [2016]. Three-dimensional free vibration analysis of carbon nanotube reinforced composites annular plates. Oriental Journal of Chemistry. 32(2):1223-33.

[6] Obitayo W, Liu T. [2012]. A review: Carbon nanotube-based piezoresistive strain sensors. J Sensors Article ID 652438, 15 pages.

[7] Dharap P, Li Z, Nagarajaiah S, Barrera E. [2004]. Nanotube film based on single-wall carbon nanotubes for strain sensing. Nanotechnol, 15(3):379.

[8] Pham GT, Park YB, Wang B. ASME Manufacturing Engineering Division 2005;16(2):987–93.

[9] Knite M, Klemenok I, Shakale G, Teteris V, Zicans J. [2007]. Polyisoprene–carbon nano-composites for application in multifunctional sensors. J Alloy Compd, 434–435(0):850-3.

[10] Kang I, Schulz MJ, Kim JH, Shanov V, Shi D. [2006]. A carbon nanotube strain sensor for structural health monitoring. Smart Mater Struct, 15(3):737.

[11] Loh KJ, Kim J, Lynch JP, Kam NWS, Kotov NA. [2007]. Multifunctional layer-by-layer carbon nanotube–polyelectrolyte thin films for strain and corrosion sensing. Smart Mater Struct , 16(2):429.

[12] Li X, Levy C, Elaadil L. [2008]. Multiwalled carbon nanotube film for strain sensing. Nanotechnol, 19(4):045501.

[13] Yamada T, Hayamizu Y, Yamamoto Y, Yomogida Y, Izadi-Najafabadi A, Futaba DN. [2011]. A stretchable carbon nanotube strain sensor for human-motion detection. Nature Nanotechnol, 6(5):296-301.

[14] Lipomi DJ, Vosgueritchian M, Tee BCK, Hellstrom SL, Lee JA, Fox CH, [2011]. Skin-like pressure and strain sensors based on transparent elastic films of carbon nanotubes. Nature Nanotechnol , 6(12):788-92.

[15] Petersen KE. Silicon as a mechanical material. Proceedings of the IEEE 1982;70(5):420-57.

[16] Vo DQ, Shin EW, Kim JS, Kim S. [2010]. Low-temperature preparation of highly conductive thin films from acrylic acid-stabilized silver nanoparticles prepared through ligand exchange. Langmuir, 26(22):17435-43.

[17] Ferrell N, Yang Y, Hansford DJ. [2010]. Micropatterning of sulfonated polyaniline using a soft lithography based lift-off process. Microsys Technol 16(11):1951-6.

[18] He Y, Wang JA, Zhang W, Song J, Pei C, Chen X. [2010]. ZnO-nanowires/pani inorganic/organic heterostructure light-emitting diode. J Nanosci Nanotechno, 10(11):7254-7.

[19] Hong SH, Bae BJ, Lee H, Jeong JH. [2010]. Fabrication of high density nano-pillar type phase change memory devices using flexible AAO shaped template. Microelectron Eng, 87(11):2081-4.

[20] Kondo Y, Tanabe H, Otake [2010]. T. Novel electrochromic polymer for electronic paper. IEICE Trans Electron, 93(11):1602-6.

[21] Martinez AW, Phillips ST, Whitesides GM, Carrilho E. [2009]. Diagnostics for the developing world: microfluidic paper-based analytical devices. Analy Chem 2009;82(1):3-10.

[22] Zhao W, Berg A. Lab on paper. Lab Chip, (8):1988-91.

[23] Clegg DL. Paper chromatography. Analy Chem 1950;22(1):48-59.

[24] Dungchai W, Chailapakul O, Henry CS. [2010]. A low-cost, simple, and rapid fabrication method for paper-based microfluidics using wax screen-printing. Analyst, 136(1):77-82.

[25] Hossain SMZ, Luckham RE, Smith AM, Lebert JM, Davies LM, Pelton RH, [2009]. Development of a Bioactive Paper Sensor for Detection of Neurotoxins Using Piezoelectric Inkjet Printing of Sol− Gel-Derived Bioinks. Analy Chem, 81(13):5474-83.

[26] Liu X, Mwangi M, Li XJ, O'Brien M, Whitesides GM. [2011]. Paper-based piezoresistive MEMS sensors. Lab Chip, 11(13):2189-96.

[27] Ren TL, Tian H, Xie D, Yang Y. [2012]. Flexible graphite-on-paper piezoresistive sensors. Sensors, 12(5):6685-94.

[28] Kosmala A, Wright R, Zhang Q, Kirby P. [2011]. Synthesis of silver nano particles and fabrication of aqueous Ag inks for inkjet printing. Material Chem Phys, 129(3):1075-80.

[29] Magdassi S. The chemistry of silver ink. Singapore: World Scientific Publishing; [2010].

[30] Tamjid E, Guenther BH. [2010]. Rheological and sedimentation behaviour of nanosilver colloids for inkjet printing. Int J Nanomanufacturing, 5(3):383-92.

[31] Mayer ABR. [2001]. Colloidal metal nanoparticles dispersed in amphiphilic polymers. Polym Adv Technol , 12(1-2):96-106.

[32] Tan H, Xue JM, Shuter B, Li X, Wang J. [2010]. Synthesis of PEOlated Fe3O4@SiO2 nanoparticles via bioinspired silification for magnetic resonance imaging. Adv Funct Mater 20(5):722-31.

[33] Liu T, Xiao Z, Wang B. [2009]. The exfoliation of SWCNT bundles examined by simultaneous Raman scattering and photoluminescence spectroscopy. Carbon, 47(15): 3529-3537.

[34] Luo S, Liu T, Wang B. [2010]. Comparison of ultrasonication and microfluidization for high throughput and large-scale processing of SWCNT dispersions. Carbon, 48(10):2992-2994.

[35] Hu N, Karube Y, Yan C, Masuda Z, Fukunaga H. [2008]. Tunneling effect in a polymer/carbon nanotube nanocomposite strain sensor. Acta Mater, 56(13):2929-2936.

[36] Hu N, Fukunaga H, Atobe S, Liu Y, Li J. [2011]. Piezoresistive strain sensors made from carbon nanotubes based polymer nanocomposites. Sensors, 11(11):10691-10723.

[37] Luo S, Liu T. [2013]. Structure-property-processing relationships of single-wall carbon nanotube thin film piezoresistive sensors. Carbon , 59:315-324

[38] Wouterse A, Luding S, Philipse AP. [2009]. On contact numbers in random rod packings. Granular Matter , 11(3):169-177.

[39] Blouwolff J, Fraden S. [2006]. The coordination number of granular cylinders. Europhys Lett, 76(6):1095-101

[4o] Philipse A P. [1996]. The random contact equation and its implications for (colloidal) rods in packings, suspensions, and anisotropic powders. Langmuir, 12(5):1127-1133.

[41] Luo S, Liu T. [2013]. Structure–property–processing relationships of single-wall carbon nanotube thin film piezoresistive sensors. Carbon , 59:315-324.

[42] Song X, Liu S, Gan Z, Lv Q, Cao H, Yan H. [2009]. Controllable fabrication of carbon nanotube-polymer hybrid thin film for strain sensing. Microelectron Eng, 86(11):2330-2333.

[43] Sickert D, Taeger S, Kühne I, Mertig M, Pompe W, Eckstein G. [2006]. Strain sensing with carbon nanotube devices. Phys Status Solidi, 243(13):3542-3545.

[44] Pham GT. [2008]. Characterization and modeling of piezo-resistive properties of carbon nanotube-based conductive polymer composites. Tallahassee FL USA, Florida State University, PhD thesis.

[45] Ando Y, Zhao X, Shimoyama H, Sakai G, Kaneto K. [1999]. Physical properties of multiwalled carbon nanotubes. Int J Inorg Mater, 1(1):77-82.

[46] Breuer O, Sundararaj U. [2004]. Big returns from small fibers: A review of polymer/carbon nanotube composites. Polym Compos, 25(6):630-45.

[47] Yang L, Anantram M, Han J, Lu J. [1999]. Band-gap change of carbon nanotubes: Effect of small uniaxial and torsional strain. Phys Rev B, 60(19):13874.

[48] Yang L, Han J. [2000]. Electronic structure of deformed carbon nanotubes. Phys Rev Lett 85(1):154-7.

[49] Heyd R, Charlier A, McRae E. [1997]. Uniaxial-stress effects on the electronic properties of carbon nanotubes. Phys Rev B, 55(11):6820.

[50] Buldum A, Lu JP. [2001]. Contact resistance between carbon nanotubes. Phys Rev B, 63(16):161403.

[51] Buia C, Buldum A, Lu JP. [2003]. Quantum interference effects in electronic transport through nanotube contacts. Phys Rev B, 67(11):113409.

[52] Simmons JG. [1963]. Generalized formula for the electric tunnel effect between similar electrodes separated by a thin insulating film. J Appl Phys, 34(6):1793-803.

[53] Theodosiou T. C, Saravanos D. A. [2010]. Numerical investigation of mechanisms affecting the piezoresistive properties of CNT-doped polymers using multi-scale models. Compos Sci Technol, 70(9):1312-1320.

[54] Luo S, Liu T, Benjamin S. M, Brooks J. S. [2013]. Variable Range Hopping in Single-Wall Carbon Nanotube Thin Films: A Processing–Structure–Property Relationship Study. Langmuir, 29(27):8694-8702.

[55] Hu N, Itoi T, Akagi T, Kojima T, Xue J, Yan C, Liu Y, [2013]. Ultrasensitive strain sensors made from metal-coated carbon nanofiller/epoxy composites. Carbon , 51: 202-212.

[56] Skakalova V, Kaiser A. B, Woo Y.S, Roth S. [2006]. Electronic transport in carbon nanotubes: From individual nanotubes to thin and thick networks. Phys. Rev. B , 74 (8): 085403

[57] Kaiser A.B, Skakalova V, Roth S. [2008]. Modelling conduction in carbon nanotube networks with different thickness, chemical treatment and irradiation.Physica E , 40 (7): 2311–2318.

ABOUT AUTHORS

Mohammadmehdi Choolaei *is Department of Tissue Engineering and Regenerative Medicine, School of Advanced Technologies in Medicine, Shahid Beheshti University of Medical sciences,Tehran,Iran and Research Institute of Petroleum Industry (RIPI), Azadi sport complex West Blvd., Tehran, Iran*

Milad Nazarzadeh *is Medical Nano-Technology & Tissue Engineering Research Center, School of Advanced Technologies in Medicine, Shahid Beheshti University of Medical sciences, Tehran, Iran*

Amir Yadegari *is Medical Nano-Technology & Tissue Engineering Research Center, School of Advanced Technologies in Medicine, Shahid Beheshti University of Medical sciences, Tehran, Iran*

Hakimeh Zali *is Medical Nano-Technology & Tissue Engineering Research Center, School of Advanced Technologies in Medicine, Shahid Beheshti University of Medical sciences, Tehran, Iran*

Fatemeh Yazdian is Faculty of New Science and Technology, University of Tehran , Tehran, Iran

Meisam Omidi is Medical Nano-Technology & Tissue Engineering Research Center, School of Advanced Technologies in Medicine, Shahid Beheshti University of Medical sciences, Tehran, Iran